Surface & Coatings Technology 437 (2022) 128317

Contents lists available at ScienceDirect

Surface & Coatings Technology

journal homepage: www.elsevier.com/locate/surfcoat

Improvements of surface tribological properties by magnetic assisted ball burnishing

Zsolt F. Kovács [a,*], Zsolt J. Viharos [a,b], János Kodácsy [a]

[a] John von Neumann University, GAMF Faculty of Engineering and Computer Science, Dep. of Innovative Vehicles and Materials, Manufacturing Technology Research Group, Faculty of Economics, Kecskemét H-6000, Hungary

[b] Institute for Computer Science and Control (SZTAKI), Centre of Excellence in Production Informatics and Control (RITT), Eötvös Loránd Research Network (ELKH), Center of Excellence of the Hungarian Academy of Sciences (HAS), Research Laboratory on Engineering and Management Intelligence, Intelligent Processes Research Group, Budapest H-1111, Hungary

ARTICLE INFO

Keywords:
Magnetic assisted finishing
Ball burnishing
Surface roughness
Surface topography
Tribology
Oil pockets

ABSTRACT

The effect of the magnetic assisted ball burnishing on a general, C45 steel was investigated considering tribological aspects. In engineering practice, the tribological properties of machined surfaces are characterized by amplitude roughness parameters from roughness profiles, as *Rpk*, *Rk*, *Rvk*, *Rsk* and *Rku*. Information about the sliding properties can be described by these parameters together with the oil retention capacity of the surface. Despite the conventional burnishing processes used as a post-machining operation, the authors applied a newly designed magnetic assisted ball burnishing method and tool, which can also burnish flat or harmonically changing surfaces and is able to round the edge of the workpiece in one pass as well, immediately after milling. To increase efficiency of the applied burnishing process, different types of burnishing strategies were applied and compared. The results of the investigations showed that the magnetic assisted ball burnishing decreases the frictional resistance, and at the same time it creates advantageous oil pockets on the machined surface.

1. Introduction

The magnetic assisted ball burnishing (MABB) is a post-machining surface finishing process, therefore it decreases the residual tension stresses on the machined surface and reduces the surface roughness, similarly to the way conventional ball/roller burnishing technologies do [1]. Meanwhile, the newly developed MABB tool is as economically beneficial, simple, and cheap as the conventional burnishing tool, because the necessary burnishing force is generated by a NdFeB neodymium magnet (Fig. 1).

When using the proposed MABB tool, the density and shape of the magnetic flux passing through the workpiece and the balls have an indirect effect on the burnishing force, which then depends on i) the diameter of the burnishing ball (d_b), ii) the magnetic field (H) and its spatial distribution, iii) the material composition and design of the tool elements and iv) the distance between the tool and the work-piece (h) [2]. The key element in the interaction between the balls and the tool is the wedge effect. In magnetizable materials, the flux of the permanent magnet, largely due to the tool design, passing through the end of the tool cone increases the gradient and attracts the balls towards the centre of the MABB tool which results in the burnishing force being oriented in the direction of the machined surface [2,3].

According to the preliminary results the maximum achievable burnishing force is 350 ± 10 N at $h = 10$ mm [3]. This value was used by the authors in the present experiment as well.

The introduced MABB tool has a number of beneficial properties over conventional technologies:

- it can round the edge in one pass with burnishing [4],
- it is easily indexable in a CNC machine and magazine holder,
- it can harmonically follow the (sometimes waving) surfaces' diversities without lifting the tool,
- it does not require any special resources (e.g. hydraulic pump, hydraulic hose, spring) thus the required burnishing force is stable and constant,
- it is maintenance-free and particularly productive thanks to the four burnishing balls (all conventional burnishing techniques apply only one ball), so it is truly economical.

More information about the MABB tool can be found in in the

* Corresponding author.
E-mail address: kovacs.zsolt@gamf.uni-neumann.hu (Z.F. Kovács).

https://doi.org/10.1016/j.surfcoat.2022.128317
Received 21 November 2021; Received in revised form 15 February 2022; Accepted 28 February 2022
Available online 4 March 2022

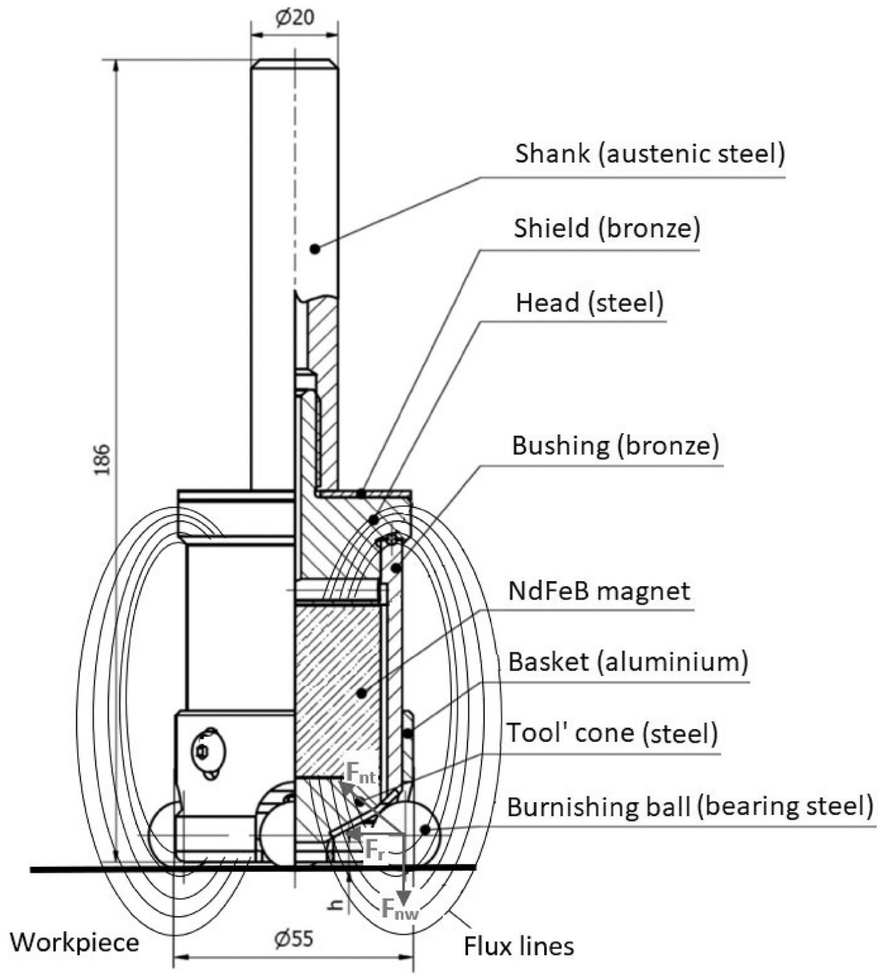

Fig. 1. Parts of MABB tool and flux lines.

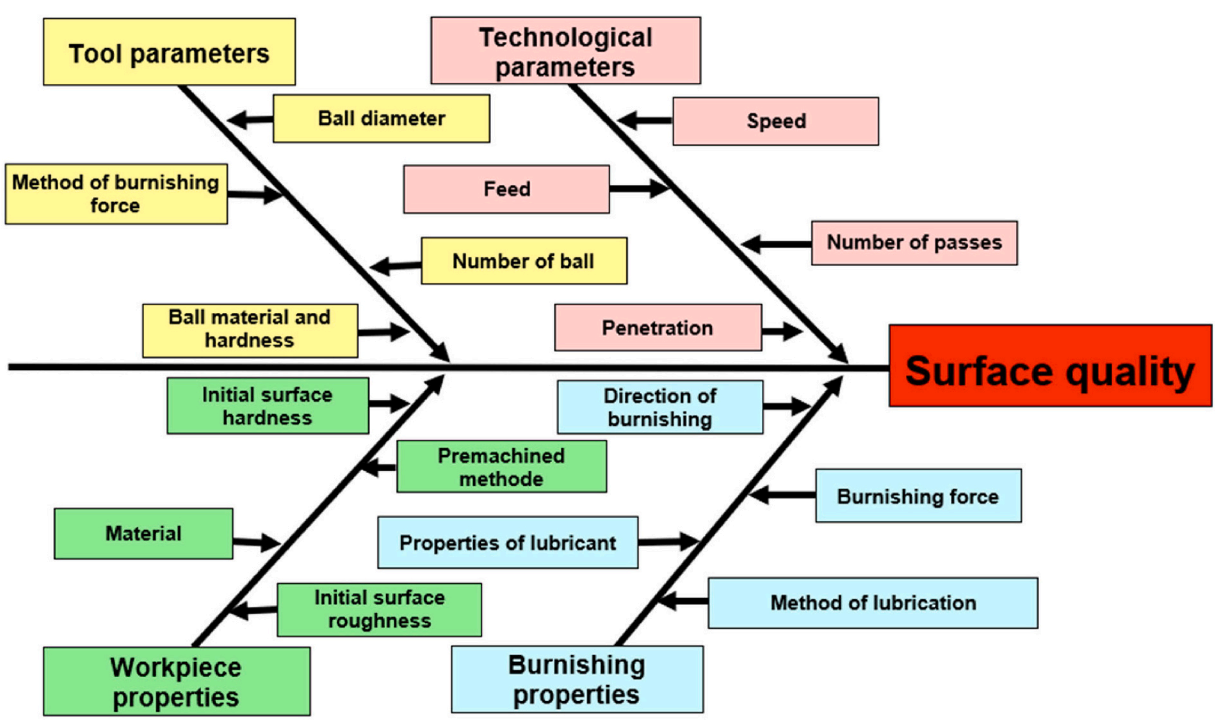

Fig. 2. Ishikawa diagram of ball burnishing.

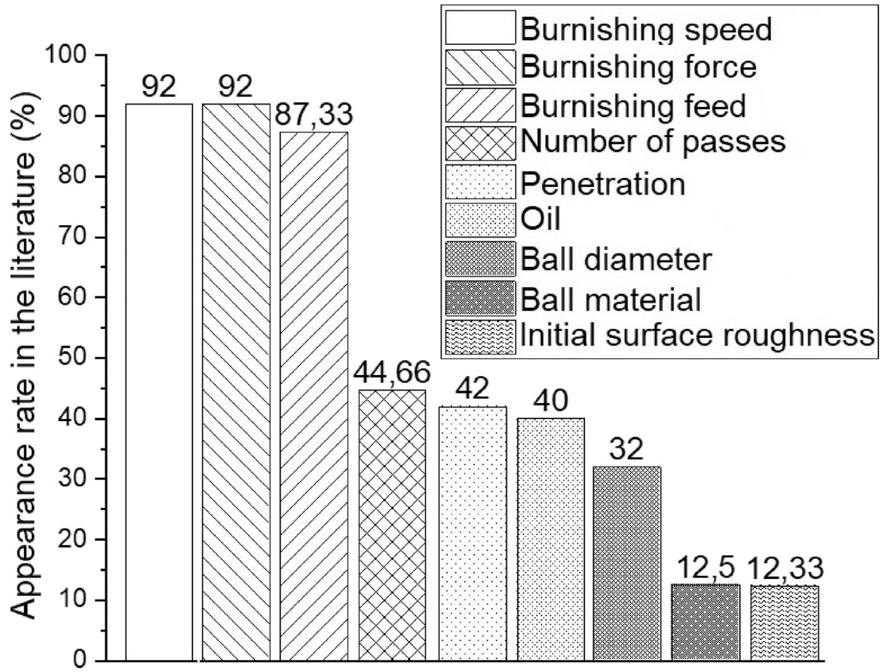

Fig. 3. Percentage of the investigated burnishing factors in the scientific literature [6].

authors' previous articles [2–5].

Ferromagnetic materials are effectively burnishable because the required burnishing force is provided by the attraction between the balls and the workpiece [2]. Additionally, nonferrous materials can also be burnished if a magnetic table or magnetic source is placed under the workpiece [2]. During burnishing, a tool – such as a face mill tool – moves along the designed path at a given feed and revolution per minute, consequently, its application in the state-of-the-art machining environment is certainly convenient.

Naturally, there are numerous ball burnishing factors and parameters which all have an effect on the surface quality, as Fig. 2 represents. Due to the variety and complexity of these influencing factors, several studies have already been conducted to optimize the factors and their parameters and to investigate their interaction with each other. Based on the survey by Maheshwari and Gawande, a diagram was presented which shows the frequency of investigations on general burnishing technologies focusing on burnishing speed, feed, and burnishing force and other important factors in the scientific literature (Fig. 3) [6]. Figs. 2 and 3 also demonstrate many other important parameters – this is the reason why optimum values had to be determined beyond speed or feed [7], such as the applied oil [8] or burnishing force level [9]. For example, too high of a burnishing force with too many burnishing passes can cause surface destruction [10,11].

In their research, Rodríguez et al. [12] came to a surprising result: increasing the burnishing force does not necessarily cause an improvement in surface roughness, moreover, in certain cases it even leads to surface deterioration, but even then, the hardness of the surface is improved. So, a very high burnishing force should only be used if the goal is surface hardening rather than roughness reduction [12].

In addition to the numerous technical advantages of ball burnishing, it has to be mentioned that this technology is environmentally friendly as well, even if oil is used during its application. As MABB is a cold forming process with continuous friction, the use of lubricating oil is essential, even though most of the literature does not mention the importance of lubricants (see Fig. 3). However, they have significant impact on surface roughness metrics and on the environmental load as well. In order to be environmentally friendly, instead of fossil oil, coconut oil can be used, which is entirely green and has the same machining results [13]. The lubricating oil can be applied to the surface by pre-lubrication or by a Minimum Quality Lubrication (MQL) system. Most of the available scientific publications examine the effects of oil types [8,9] but not the method by which the oil is delivered, although this factor can be pivotal from economic and environmental aspects.

Based on further reported observations, it can be stated that ball burnishing is suitable for improving the surface wear resistance and the tribological properties [14], which cause good wettability [15,16] as well. Surface quality, however, is one of the most important and most characteristic evaluation parameters of machinability [17,18].

Tillmann et al. [19] investigated the usable life of the surface. As a result, the surface lifetime increases to about one and a half times more due to burnishing [19]. Hiegemann et al. achieved similar results, while surface roughness was also improved [20].

The current paper evaluates the newly introduced MABB technique focusing on the essential tribological aspect and shows the superiority of this technology over many other surface engineering techniques.

2. Tribology evaluation of machined surfaces

In the engineering sciences, it is generally accepted that for steels and metals surface roughness values are closely related to their corrosion resistance [21] because the rate of corrosion decreases alongside the effective contact surface size [22–24]. Furthermore, the surface roughness and microgeometry of surfaces have great effect on the wearing and sliding performance properties of the material [25,26]. It is similar to the laser formed [27,28] or plasma sprayed surfaces [29], however, the burnishing is far less expensive. Therefore, certain types of coating technologies [25] can improve the tribological and corrosion properties, but the magnetic assisted ball burnishing is also able to produce a high-quality surface as well. The word "tribology" is derived from the two Greek words 'tribos' (burnish) and 'logos' (tenet), so it literally means 'burnish tenet'. In 1968, the German Society of Tribology defined the science of tribology as follows [30]:

> "*Tribology is the science of scientific research and practical application of regularities and knowledge in the fields of friction, wear and lubrication.*"

Because the tribological properties are highly dependent on the

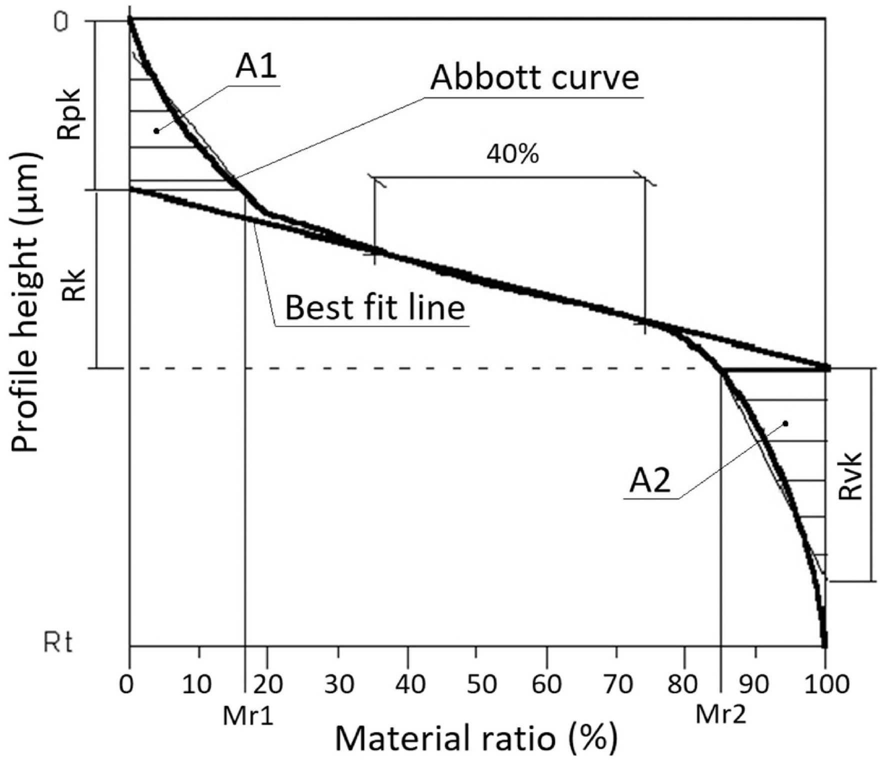

Fig. 4. Interpretation of the *Rpk*, *Rk* and *Rvk* parameters from the Abbott curve by ISO 13565-2 [47].

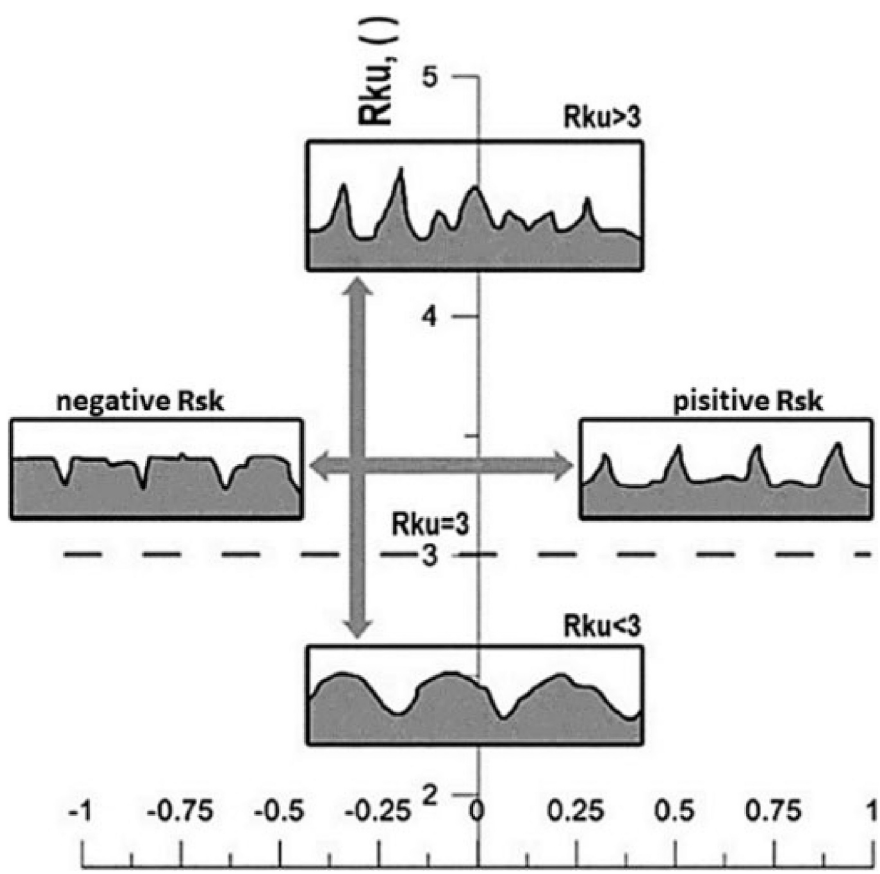

Fig. 5. Interpretation of Rsk and Rku amplitude parameters [53].

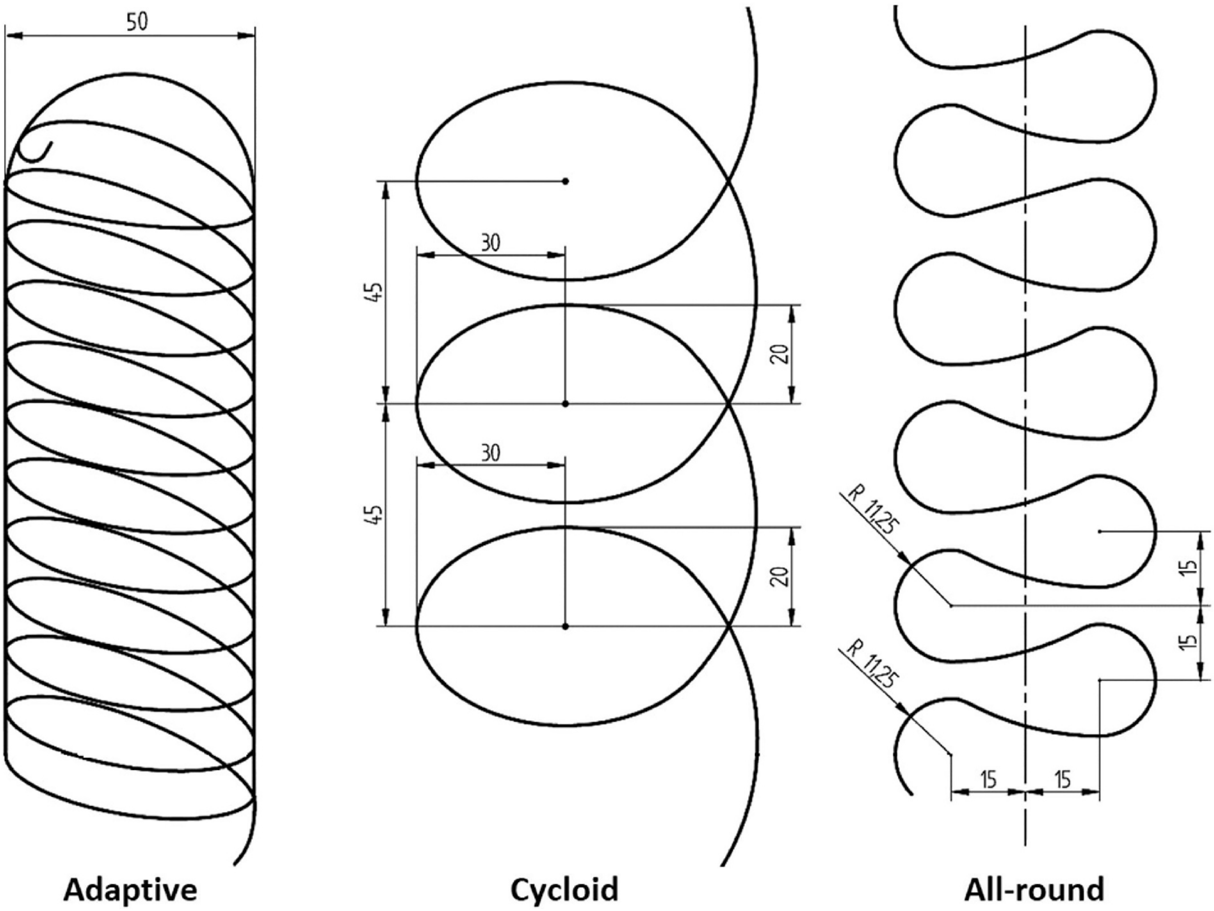

Fig. 6. Tool paths of the first three burnishing strategies.

surface quality of the workpiece [31,32], technologies e.g. ball burnishing are adequate for creating tribologically suitable surfaces [33,34]. This surface quality is characterized by surfaces which have good sliding properties and appropriate oil retention [33]. Sliding properties can be determined by wear tests [35,36], but it is also a common method to analyse them by profilometric measurements. In doing so, the surface of the test piece is scanned using a contact or contactless method. In this case, during the tribological measurement, the R profile of the surface is recorded and evaluated by the related amplitude roughness parameters, which are the following [37,38]:

Rpk: peak height – characterizes the size of the fast-wearing layer,
Rk: core height of profile – characterizes the surface life,
Rvk: reduced valley depth – from which the retention capacity of lubricant and debris can be deduced,
Rsk: skewness parameter – measures the asymmetry of the surface profile,
Rku: flatness parameter (kurtosis) – indicates the “sharpness” and “peak” of the amplitude distribution of the surface curve.

In the case of sliding elements, it is important to use lubricants to reduce friction and wear between the surfaces. The problem is not primarily the application of the lubricants, but their retention on the surface, because they can disappear during the movements, which results in dry friction [39]. To prevent this, scratch marks (oil pockets) of designed geometry are intentionally created on the surface to ensure oil retention [40,41]. There are several methods for creating as many scratch marks as needed to improve the tribological properties, e.g., peeling [42], honing [43], laser surface treatment [44,45], electrochemical machining[46] or plastic burnishing process [34].

The oil retention valley (A2) is characterized by the parameters of *Rpk*, *Rk* and *Rvk* which are defined by the ISO 13565-2 standard. These are derived from the Abbott curve, as shown in Fig. 4 [47].

These important, general, and industry-standard roughness parameters are used effectively for characterization of cylinder holes in motors [48], gear contact surfaces [49], and all surfaces where surface oil retention is expected [50]. Oil-bearing scratches can also be examined with measured S-profiles of surfaces according to ISO 25178-2 [51], as they clearly show the individual grooves and their structures [52]. Being aware of the related, so called A2 parameter (see Fig. 4) is especially important because it gives the intensity of surface re-oiling. However, the most important tribological indicators are the amplitude *Rsk* and *Rku* parameters, which are used for positioning the different machined surfaces in a diagram to obtain comparable results on the tribological characteristics of them. The science of tribology calls this diagram “tribological topographic map” [53] with the experimental values of *Rsk* and *Rku*.

The *Rsk* parameter shows the shape of the height distribution of the profile and its asymmetry with respect to the centre line. Its value is positive if the peaks of the surface profile are greater than the depths of the valleys and its value is negative if the valleys are deeper than the magnitude of the peaks. Fig. 5 shows that the surface is “sharper” when the value is positive. Negative *Rsk* values indicate that the machined surface texture has good load-bearing capacity and is more wear-resistant, so, this parameter carries an essential technical and practical meaning of real working surfaces [37].

The *Rku* amplitude roughness profile parameter can be advantageously used to predict the wear behaviour of machined surfaces. In its evaluation, it is examined whether its value is greater or less than 3. If $Rku > 3$, the sliding surfaces are characterized by intense wear, and if

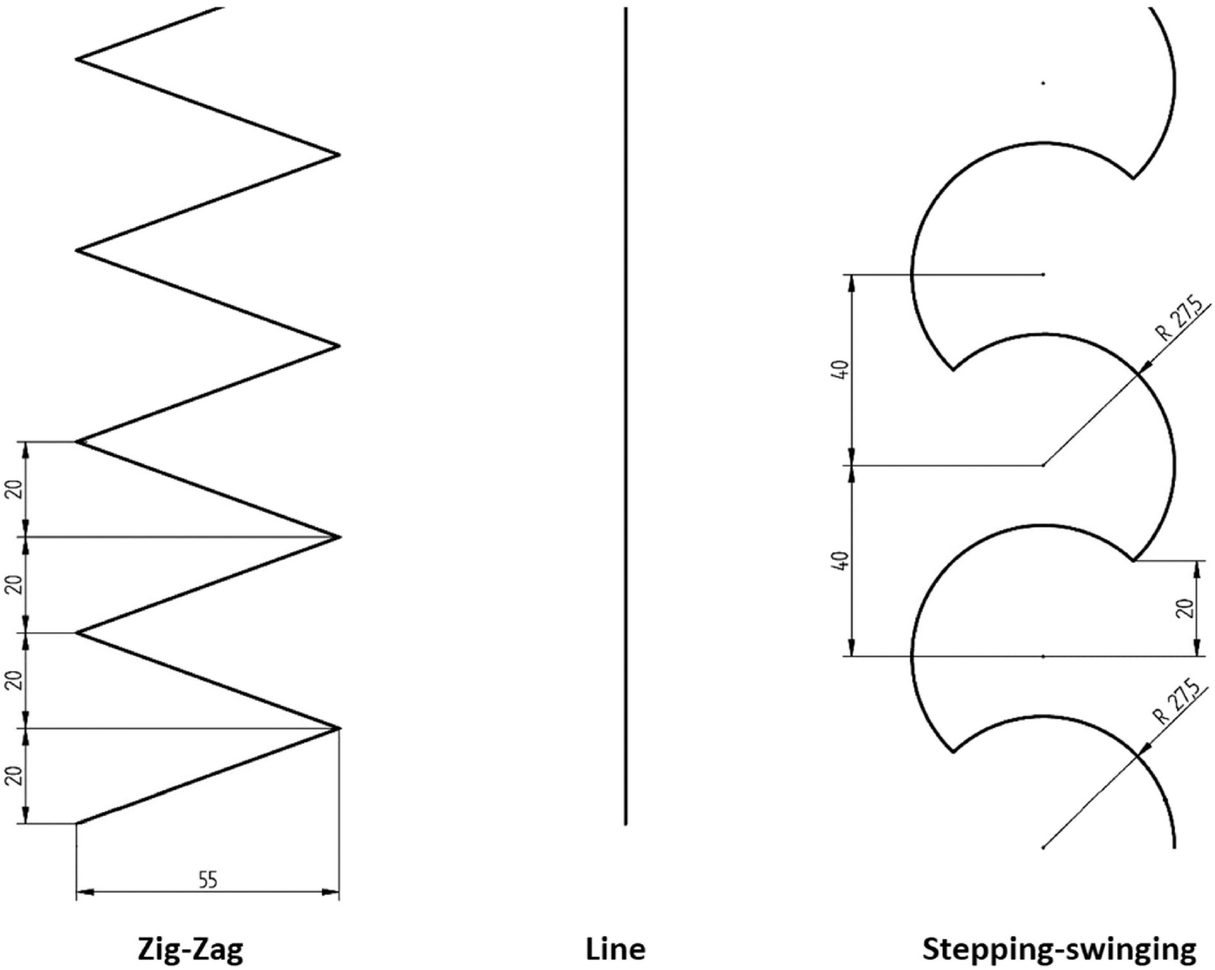

Fig. 7. Tool paths of the second three burnishing strategies.

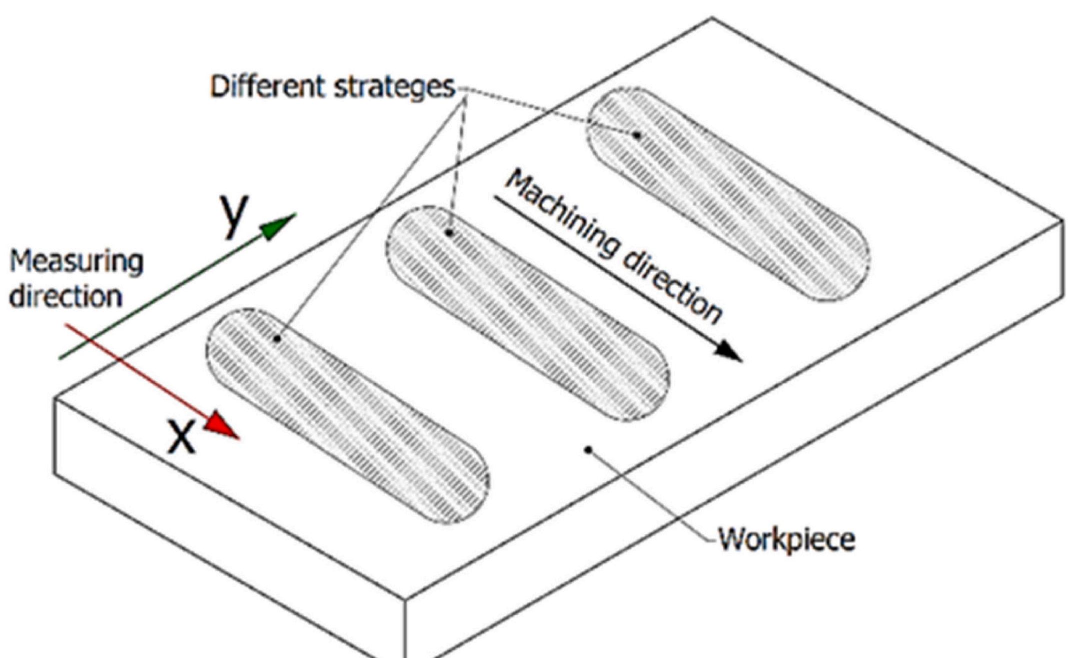

Fig. 9. Roughness profiles and Abbott curve of milled and burnished surfaces.
(0-Milled, 1-Adaptive, 2-Cycloid, 3-All-round, 4-Zig-zag, 5-Line, 6-Stepping-swinging.)

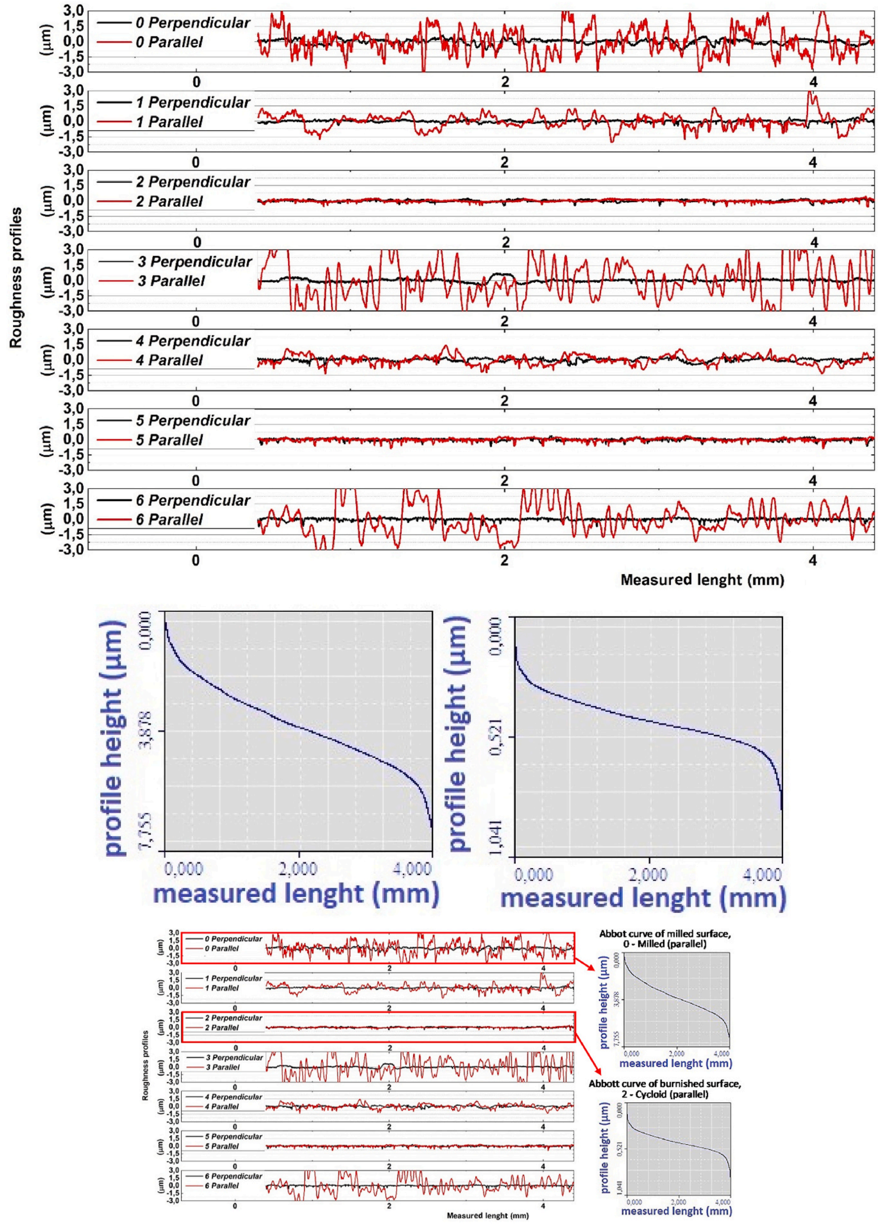

Fig. 8. The measuring directions of the roughness of each burnishing strategy.

Rku < 3, the distribution of surface irregularities is more favourable, in this case, the profile can be said to be filed and more resistant (Fig. 5) [52].

3. Experiments for tribological evaluation

The MABB tool used in the experiments is suitable for burnishing with similar strategies to those technologies that are used for milling on a typical CNC machine [54,55] due to its beneficial design.

The authors investigated the effects of each machining strategy on the resulted surface quality by evaluating the experiments. To generate various strategies, both the built-in CAM (Computer Aided Manufacturing) strategies available in the Autodesk Inventor HSM® and also self-generated paths were used. They represent the state-of-the-art typical tool path generation solutions. The burnishing experiments were performed on a 270 × 170 × 35 mm C45 steel which was face (pre) milled with eight pieces of SECO APMX160408TR-M14 MP2500 milling inserts. The direction of the milling was the same as the direction of the burnishing. The technological parameters of burnishing were constant for each strategy, the optimal values were determined by the authors earlier, so the following parameters were applied in the actual research: $v_b = 40$ m/min, $v_f = 50$ mm/min and $h = 10$ mm where the measured burnishing force was 350 ± 10 N [54]. A total of six MABB tool path strategies (*1-Adaptive*, *2-Cycloid*, *3-All-round*, *4-Zig-zag*, *5-Line* and *6-Stepping-swinging*) were tested, the scaled drawings and names of which are shown in Figs. 6 and 7, where the lines indicate the trajectory of the centre of the tool.

4. Results and discussions

After the ball burnishing processes, all the machined surfaces on the workpiece of C45 material were evaluated by registering the surface profile and calculating the surface roughness.

The following measuring equipment was used throughout the experimental work: for 2D surface measurements a MITUTOYO Formtracer SV-C3000 and for 3D surface measurements a MarSurf XCR20 CT200Mot with CNC table. Measurements were carried out with the ISO 13565-1:2000 calculation method where the evaluation length was $l_m =$

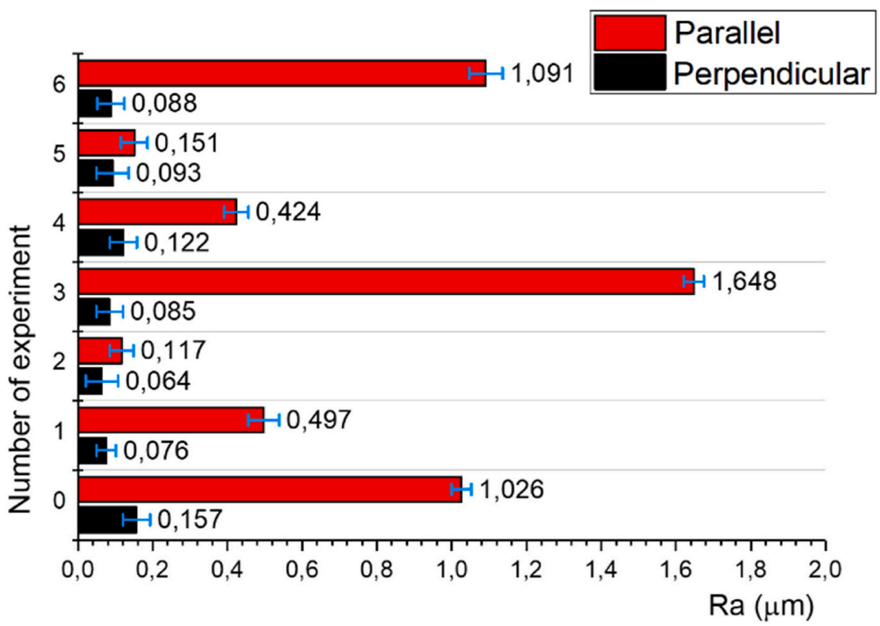

Fig. 10. Comparison of Ra roughness of milled and different burnished strategies in perpendicular (black) and parallel (red) measuring direction from the machined direction.
(0-Milled, 1-Adaptive, 2-Cycloid, 3-All-round, 4-Zig-zag, 5-Line, 6-Stepping-swinging.) (For interpretation of the references to color in this figure legend, the reader is referred to the web version of this article.)

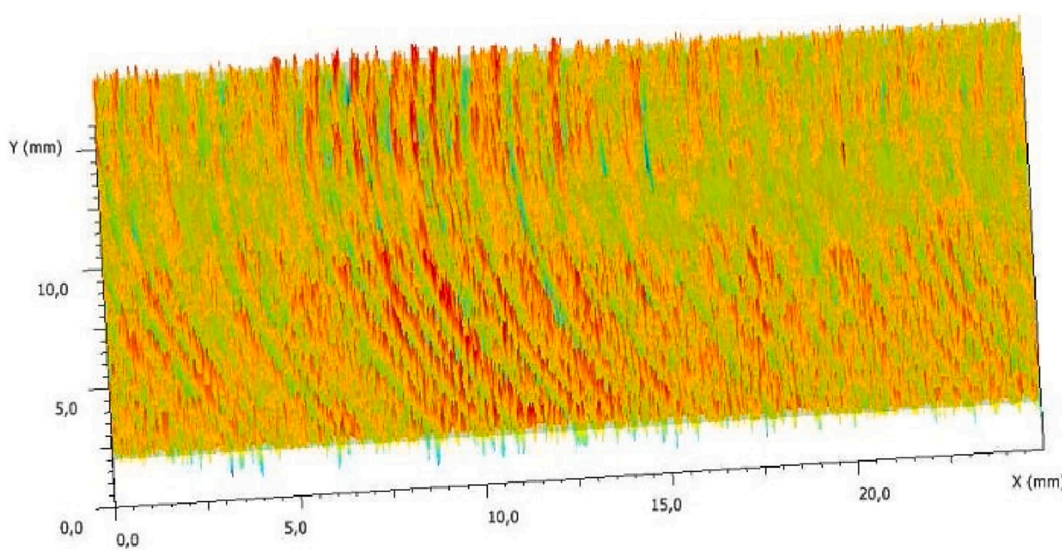

Fig. 11. Topographical mapping of surface roughness analysis on the initial milled surface.

4 mm, lower cut-off was λc = 0.8 mm and upper cut-off was λs = 0.0025 mm (which fits the measured range of the roughness according to the standard).

As the structure of the burnished surfaces is different (because of the direction and range of the strategies) the roughness measurement was performed in two directions. One measurement was performed parallel to the machining direction (perpendicular to the original scratch marks generated by the pre-milling), while the other measurement was performed perpendicular to the machining direction (parallel to the original scratch marks) [56]. Each machined surface was scanned three times in both directions and the averages of them were used in the evaluation. A schematic arrangement of the measurements is shown in Fig. 8.

The measurements were performed not only on the burnished surfaces, but also on the original milled surface, which is hereinafter denoted by an index of 0-Milled. The milled (0) and burnished (1–6) *R* profiles recorded during the roughness measurement are shown in Fig. 9, where the red graph indicates the parallel measuring direction and the black graph indicates the perpendicular measuring direction to the machining direction. Based on Fig. 9, it can be stated that the roughness profiles are smoother measured perpendicular to the machining direction. This is due to the fact that the direction of machining of the face milling before burnishing was the same as the direction of travel of the burnishing, so the scratch marks formed at that time affect the quality of the burnished surface and no significant change is observed here. Measuring parallel to the machining direction, a larger difference can already be observed between milled and burnished surfaces. The Abbott curves of milled surfaces (0-Milled) show (Fig. 9) that they have a higher profile height in the case of the burnished surface (2-Cycloid) and the slope of the curve is also much higher. It means that the intensity of wear is much faster in case of sliding elements.

4.1. *Effect on the surface roughness*

From a tribological point of view, in addition to the described amplitude indicators, the *Ra* roughness parameter is also important, because in the case of sliding surfaces, the surfaces with coarse

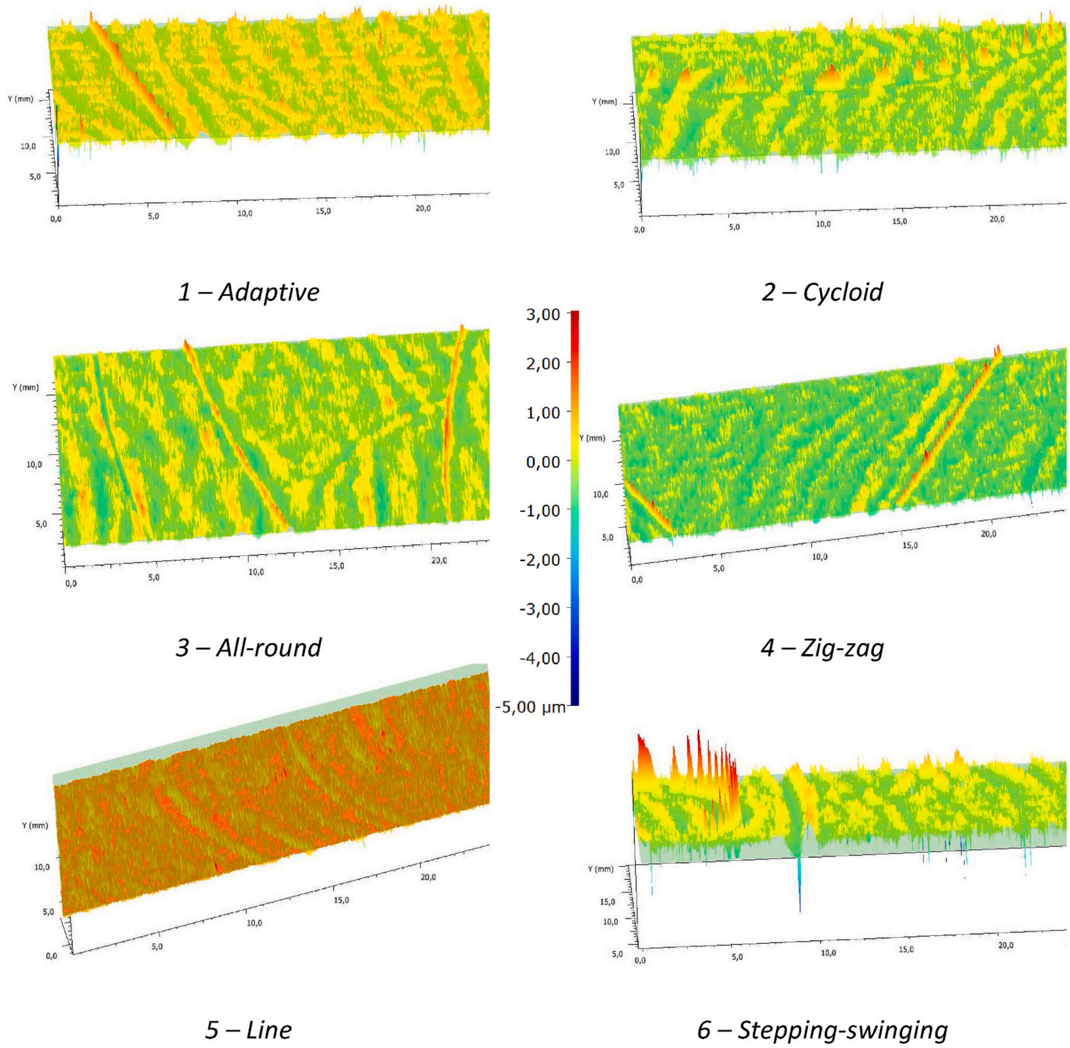

Fig. 12. Topographical 3D maps of the burnished surfaces with different strategies (the territory of the measured area is 15 × 25 mm).

roughness wear each other, while surfaces that are too fine can have a so-called stick-slip effect, which comes from the surfaces sticking together [37]. Naturally, the *Ra* roughness parameter alone is not suitable for judging tribological properties, but together with amplitude indicators, they already give a comprehensive result that is widely applied in industry.

Similar to Fig. 9, Fig. 10 also adequately represents that the change in roughness values is smaller when the measurement accounts for the perpendicular direction.

To examine the roughness changes, let us consider the *Ra* roughness of the milled surface as 100% and compare the resulted *Ra* roughness of the different burnishing strategies, which are divided into groups of perpendicular and parallel to the machining direction. Based on this evaluation, the following conclusions can be drawn:

The surface machined with the "2-Cyclois" strategy improved the most in both directions. The Ra roughness decreased by 89.1% in the parallel and by 59.2% in the perpendicular directions.

The "3-All-round" and "6-Stepping-swinging" strategies deteriorated the average surface roughness in the parallel direction (3 → 60%; 6 → 6.3%) but improved in the perpendicular direction (3 → 45.9%; 6 → 43.9%).

That surface which was burnished with the "5-Straight" strategy shows a great improvement in the parallel direction, its value being 85.3%, and there is also an improvement in the perpendicular direction of 40.8%.

The "4-Zig-zag" strategy produced the smallest improvement in the perpendicular direction, which became 22.3%. In parallel direction it improved the *Ra* by 58.7%.

In the case of "1-Adaptive" strategy, the decrease is 51.6% in both directions.

4.2. Influence on the oil holding capacity

The oil holding capacity of the machined workpieces are evaluated based on the *Rk*, *Rpk* and *Rvk* parameters from the Abbott curve (Fig. 4) [47]. This evaluation also required the values of Mr1 and Mr2 indicators, because the *Rvk* parameter only gives the depth of the oil-bearing valleys and does not characterize the amount of oil that can be retained. Mr1 is the Material Ratio corresponding to the upper limit position of the roughness core and the Mr2 is the Material Ratio corresponding to the lower limit position of the roughness core (Fig. 4).

The area between the Material Ratio Curve and the lower intersection line is the size of the oil retention valleys (A2); it can be calculated as the area of a right-angled triangle of base length Mr2 to 100% and height *Rvk* in Eq. (1) [47].

$$\mathrm{A2} = \frac{1}{2} \bullet \frac{\mathrm{Rvk} \bullet (100\% - \mathrm{Mr2})}{100\%} \tag{1}$$

The original milled and the burnished surfaces' values of *Rk*, *Rpk*, *Rvk*, Mr1, Mr2 and A2 are summarized in Table 1.

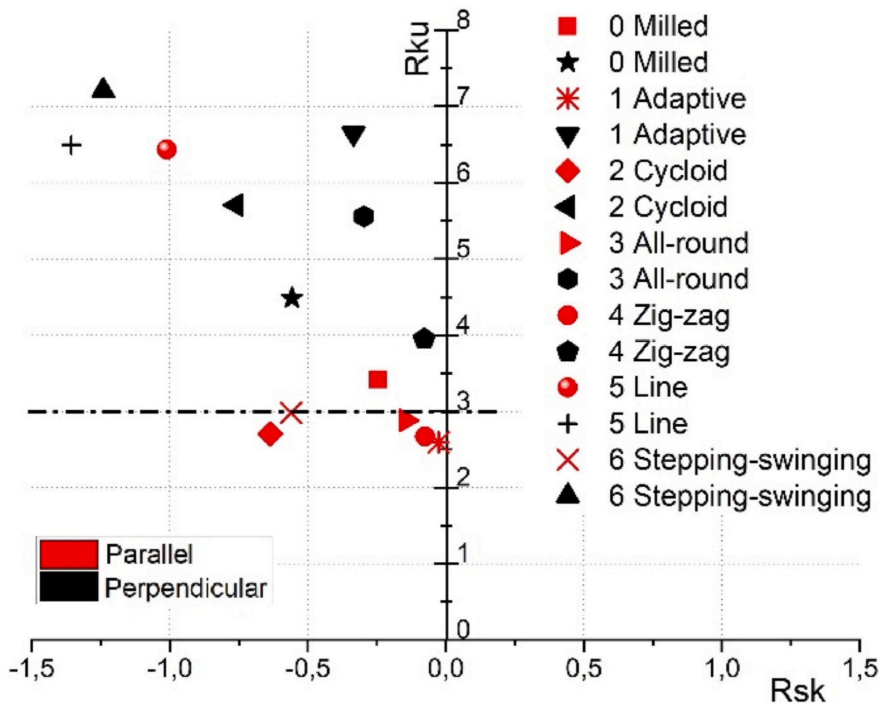

Fig. 13. *Rsk-Rku* topographic map of milled (0) and differently burnished (1–6) surfaces.

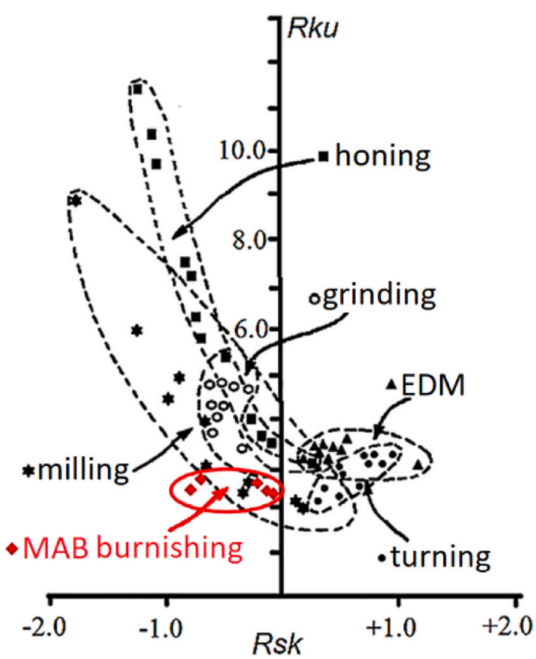

Fig. 14. MABB burnishing locations on the *Rsk-Rku* topographic map [49].

According to Table 1, the value of the *Rvk* parameter in the parallel direction in the case of "3 – All-round" strategy is the largest, while measured in the perpendicular direction, the "6 – Stepping-swinging" strategy has the largest *Rvk* value.

Considering solely the A2 values, it can be concluded that using these two strategies (3 – All-round and 6 – Stepping-swinging), the highest A2 value can be measured, which means those surfaces made with these two burnishing strategies can hold the highest amount of oil.

After milling, the surface integrity is favourable in terms of oil retention (Table 1), but as Fig. 11 shows, it contains lots of sharp and high peaks, which results in a surface unsuitable for sliding [57]. This phenomenon proves that the A2 does not specify the sliding properties, so a low value of A2 does not mean an inferior sliding property. In order to be able to correctly assess the sliding property, familiarity with the Rsk and Rku parameters is essential [58,59].

Topographical 3D maps of the burnished surfaces show the oil retaining grooves, reflect the shapes of the burnishing strategy and show the achieved flatness of the roughness peaks (Fig. 12). According to Fig. 12, the "2 – Cycloid", "4 – Zig-zag" and "3 – All-round" strategies have tribologically advantageous surfaces, while the "5 – Line" is the worst option.

Based on this experimental setup, the oil retention capacity can be quantified (Table 1), thus it can be concluded that tribologically significant oil-retaining valleys remained on the burnished surfaces (made with the novel MABB tool).

4.3. Tribological properties

After the analysis of *Ra*, *Rk*, *Rpk*, *Rvk* and A2, the values of the amplitude *Rsk* and *Rku* (Table 2) markers can be placed on the topographic map as shown in Fig. 13, where the parallel machining direction of the MABB tool is indicated by red markings and the perpendicular direction is indicated by black markings.

Based on Fig. 13, the following main observations can be recognized:

Each strategy has a negative *Rsk* value, which means that the roughness peaks are blunt, therefore the contact surface is increased.

From a tribological point of view, the machining direction of the MABB tool has a significant effect. The parallel direction is more favourable, which is preferred from a practical point of view, as it is the same as the machining direction of the MABB tool, so long surfaces can be machined with the proposed technology.

The "2 – Cycloid", Stepping-swinging, "3 – All-round", "4 – Zig-zag" and "1 – Adaptive" strategies (measured parallel to the machining direction of the MABB tool) result in tribologically sufficient surfaces, while the "5 – Line" strategy is less suitable from this point of view.

The "2 – Cycloid" strategy results in the most favourable surface because the *Rsk* value is the smallest (*Rsk* = −0.636) and the *Rku* value is

Table 1
Values of *Rk*, *Rpk*, *Rvk*, Mr1, Mr2 and A2 of the milled and the burnished surfaces with different strategies.

Strategy	Measuring direction	*Rk* (μm)	*Rpk* (μm)	*Rvk* (μm)	Mr1 (%)	Mr2 (%)	A2 (μm·%)
0 – Milled (initial surface)	Perpendicular	0.458	0.163	0.364	7.525	75.358	4.483
	Parallel	3.449	1.132	1.306	11.075	92.375	4.979
1 – Adaptive	Perpendicular	0.233	0.121	0.215	9.617	88.829	1.199
	Parallel	1.54	0.865	0.767	10.321	84.87	5.804
2 – Cycloid	Perpendicular	0.211	0.068	0.149	9.425	86.947	0.972
	Parallel	0.249	0.108	0.175	12.603	90.354	0.842
3 – All-round	Perpendicular	0.306	0.354	0.184	11.901	88.857	1.023
	Parallel	5.21	3.414	2.008	11.339	92.055	7.977
4 – Zig-zag	Perpendicular	0.329	0.069	0.251	7.717	84.309	1.973
	Parallel	1.275	0.444	0.385	7.957	92.004	1.54
5 – Line	Perpendicular	0.216	0.085	0.223	8.522	83.397	1.852
	Parallel	0.292	0.116	0.274	11.683	86.325	1.871
6 – Stepping-swinging	Perpendicular	3.257	2.467	1.517	15.825	89.871	1.519
	Parallel	0.197	0.059	0.221	10.173	86.233	7.684

Table 2
Values of *Rsk* and *Rku* amplitude parameters.

Strategy	*Rsk* ( )		*Rku* ( )	
	Parallel	Perpend.	Parallel	Perpend.
0 – Milled	−0,244	0,558	3,416	4,485
1 – Adaptive	−0,026	−0,335	2,593	6,642
2 – Cycloid	−0,636	−0,760	2,702	5,707
3 – All-round	−0,144	0,297	2,88	5,557
4 – Zig-zag	−0,075	−0,079	2,667	3,950
5 – Line	−1,011	−1,357	6,434	6,497
6 – Stepping-swinging	−0,561	−1,242	2,980	7,209

the second lowest (*Rku* = 2.702), so this can be placed on the most prominent position on the topographic map.

Considering the results of the *Ra* roughness measurement (Fig. 10), the surface made with “2 – Cycloid” strategy has the smallest Ra roughness, which further strengthens the prominent position of this strategy.

Overall, the effect of applied burnishing strategies for the surface are excellent in the tribological aspect, furthermore the “2 – Cycloid” strategy is the most suitable in terms of both tribological aspect and surface roughness.

5. Conclusions

The introduced, novel Magnetic Assisted Ball Burnishing (MABB) tool applied for machining with different burnishing strategies (*1 – Adaptive*, *2 – Cycloid*, *3 – All-round*, *4 – Zig-zag*, *5 – Line* and *6 – Stepping-swinging*) has a significant positive effect on the *Rsk* (skew parameter) and *Rku* (flatness parameter) indicators characterizing the tribological properties of surfaces. Non-straight burnishing strategies also have a beneficial effect on the *Ra* surface roughness. Surface roughness results are better without a rough change of direction in the strategy path (e.g. in the case of *2-Cyclois*, *5-Line*).

From a tribological point of view, the burnishing of C45 steel is the most favourable – the “2 – Cycloid” trajectory providing the best results among the studied burnishing strategies – with the values:

$$Rsk = -0.636 \ \mu m; \ Rku = 2.702 \ \mu m \text{ and } Ra = 0.076 \ \mu m.$$

The applied burnishing strategies with the introduced MABB tool are only appropriate in parallel machining direction, considering a tribological aspect. The measured *Ra* surface roughness values in the perpendicular direction are also favourable, but the *Rku* amplitude indicator is greater than 3, so the use of sliding elements moving in perpendicular direction is not advantageous. Meanwhile, in the parallel direction the MABB burnishing produces excellent tribological surfaces, as represented in Fig. 14.

Fig. 14 clearly represents the superior position of the introduced MABB burnishing technology. It is in the best place in the topographic map performing better than all of the other machining and finishing technologies, considering the tribological capabilities of the machined surfaces.

The introduced magnetic assisted ball burnishing can trigger the grinding and peeling in the case of sliding elements (e.g. sliding sledges), if the shape and position accuracy of the pre-machined surface are within the specified limits.

With the proposed MABB tool the machining creates oil-bearing pockets immediately after milling in one process, thus positively influencing the lubrication of the resulted surfaces.

Due to the flexible ball mounting, the technology is sensitive to dense (*1-Adaptive*, *3-All-round*) and “angular”, non-rounded (*4-Zigzag*, *6-Stepping-swinging*) changes of direction, which is apparent in the resulting higher surface roughness.

If productivity (processing time per machining area) and the resulting surface roughness are taken into account, the *5-Line* strategy is advisable, even if *2-Cyclois* results in a slightly better surface. An additional advantage of the *5-Line* is that it does not require a CNC machine.

CRediT authorship contribution statement

Zsolt F. Kovács: Conceptualization, Writing – original draft, Visualization, Investigation. **Zsolt J. Viharos:** Writing – review & editing. **János Kodácsy:** Supervision.

Declaration of competing interest

The authors declare that they have no known competing financial interests or personal relationships that could have appeared to influence the work reported in this paper.

Acknowledgements

This research is supported by EFOP-3.6.1-16-2016-00006 “The development and enhancement of the research potential at John von Neumann University” project. The Project is supported by the Hungarian Government and co-financed by the European Social Fund.

References

[1] Gy. Varga, V. Ferencsik, Investigation of the influence of different burnishing parameters on shape correctness and residual stresses, in: 23rd International Conference on Manufacturing (Manufacturing 2018), 2018. Paper: 012016.

[2] Zs.F. Kovács, Zs.J. Viharos, J. Kodácsy, Surface flatness and roughness evolution after magnetic assisted ball burnishing of magnetizable and non-magnetizable materials, Measurement 158 (2020), 107750.

[3] Zs.F. Kovács, Zs.J. Viharos, J. Kodácsy, Determination of the working gap and optimal machining parameters for magnetic assisted ball burnishing, Measurement 118 (2018) 172–180.

[4] J. Kodácsy, J. Líska, Magnetic assisted roller burnishing and deburring of flat metal surfaces, Adv. Mater. Res. 472–475 (2012) 908–911.
[5] J. Kodácsy, J. Danyi, G. Ziaja, Apparatus and method for deburring and roller-burnishing machine parts, in: Kecskemét (HU) Patent EP 1 727 648 B1, 2005, 24 02.
[6] A.S. Maheshwari, R.R. Gawande, The role of burnishing process in manufacturing industry, Int. J. Eng. Res. Dev. 13 (2017) 50–60.
[7] R. Jerez-Mesa, J.A. Travieso-Rodríguez, Y. Landon, G. Dessein, J. Lluma-Fuentes, V. Wagner, Comprehensive analysis of surface integrity modification of ball-end milled ti-6Al-4V surfaces through vibration-assisted ball burnishing, J. Mater. Process. Technol. 267 (2019) 230–240.
[8] T. Morimoto, Effect of lubricant fluid on the burnishing process using a rotating ball-tool, Tribol. Int. 25 (1992) 99–106.
[9] S. Swirad, P. Pawlus, The effect of ball burnishing on tribological performance of 42CrMo4 steel under dry sliding condition, Materials 13 (2020) 2127.
[10] A.M. Hassan, H.F. Al-Jalil, A.A. Ebied, Burnishing force and number of ball passes for the optimum surface finish of brass components, J. Mater. Process. Technol. 83 (1998) 176–179.
[11] M.H. El-Axir, An investigation into roller burnishing, Int. J. Mach. Tools Manuf. 40 (2000) 1603–1617.
[12] A. Rodríguez, L.N. López de Lacalle, A. Celaya, A. Lamikiz, J. Albizuri, Surface improvement of shafts by the deep ball-burnishing technique, Surf. Coat. Technol. 206 (2012) 2817–2824.
[13] B. Sachin, S. Narendranath, D. Chakradhar, Sustainable diamond burnishing of 17–4 PH stainless steel for enhanced surface integrity and product performance by using a novel modified tool, Mater. Res. Express 6 (2019), 046501.
[14] N.S.M. El-Tayeb, K.O. Low, P.V. Brevern, Enhancement of surface quality and tribological properties using ball burnishing process, Mach. Sci. Technol. 12 (2015) 234–248.
[15] L. Qin, P. Lin, Y. Zhang, G. Dong, Q. Zeng, Influence of surface wettability on the tribological properties of laser textured Co–Cr–Mo alloy in aqueous bovine serum albumin solution, Appl. Surf. Sci. 268 (2013) 79–86.
[16] K. Kun, Z. Weltsch, Effect of femtosecond-laser-structured injection molding tool on mechanical properties of the manufactured product, Polymers 13 (2021) 2187.
[17] V. Csala, T. Szalay, B. Farkas, S. Markos, Application benchmark of three micro hole machining processes for manufacturing the nozzle of a medical water jet machine, Acta Polytech. Hung. 12 (2015) 53–69.
[18] M. Czampa, I. Biró, T. Szalay, A novel machinability test for determining the cutting behaviour of iron-based, carbon-containing and copper-containing powder metallurgy steels (PMS), Int. J. Adv. Manuf. Technol. 89 (2017) 3495–3507.
[19] W. Tillmann, P. Hollingsworth, I. Baumann, L. Hiegemann, C. Weddeling, A. E. Tekkaya, S. Rausch, D. Biermann, Thermally sprayed finestructured WC-12Co coatings finished by ball burnishing and grinding as an innovative approach to protect forming tools against wear, Surf. Coat. Technol. 268 (2015) 134–141.
[20] L. Hiegemann, C. Weddeling, B.N. Khalifa, A.E. Tekkaya, Prediction of roughness after ball burnishing of thermally coated surfaces, J. Mater. Process. Technol. 217 (2015) 193–201.
[21] L. Jinlong, L. Hongyun, X. Jinpeng, Experimental study of corrosion behavior for burnished aluminum alloy by EWF, EBSD, EIS and raman spectra, Appl. Surf. Sci. 273 (2013) 192–198.
[22] A. Saldaña-Robles, H. Plascencia-Mora, E. Aguilera-Gómez, A. Saldaña-Robles, A. Marquez-Herrera, J.A. Diosdado-De La Peña, Influence of ball-burnishing on roughness, hardness and corrosion resistance of AISI 1045 steel, Surf. Coat. Technol. 339 (2018) 191–198.
[23] M. Salahshoor, Y.B. Guo, C. Li, Surface integrity and corrosion performance of biomedical magnesium-calcium alloy processed by amplitude dry cutting-finish burnishing, Procedia Manuf. 10 (2017) 467–477.
[24] Zs.F. Kovács, Zs.J. Viharos, J. Kodácsy, The effect of magnetic assisted ball burnishing on the corrosion resistance of C45 steel, in: dvances in Manufacturing Engineering and Materials II, Springer International Publishing, 2021, pp. 236–248.
[25] L. Li, Z. Lu, J. Pu, B. Hou, Investigating the tribological and corrosive properties of MoS2/Zr coatings with the continuous evolution of structure for high-humidity application, Appl. Surf. Sci. 541 (2021), 148453.
[26] B.Z. Balázs, T. Márton, Experimental investigation of the influence of cutting parameters on surface quality and on the special characteristics of micro-milled surfaces of hardened steels, Proc. Inst. Mech. Eng. C J. Mech. Eng. Sci. (2021), https://doi.org/10.1177/09544062211013064.
[27] J. Hlinka, M. Berczeli, G. Buza, Z. Weltsch, Wetting properties of nd: YAG laser treated copper by SAC solders, Soldering Surf. Mt Technol. 29 (2017) 69–74.
[28] J. Hlinka, Z. Fogarassy, Á. Cziráki, Z. Weltsch, Wetting properties, recrystallization phenomena and interfacial reactions between laser treated cu substrate and SAC305 solder, Appl. Surf. Sci. 501 (2020), 144127.
[29] Z. Zou, Y. Wang, F. Zhou, L. Wang, S. Liu, Y. Wang, Tribological property of plasma-sprayed Al2O3-13wt%TiO2coatingsonto resin-based composites, Appl. Surf. Sci. 431 (2018) 75–80.
[30] J. Baudner, Die bedeutung der tribologie für die instandhaltung, Stahl Eisen 124 (2004) 61–65.
[31] T. Hudec, M. Mikula, L. Satrapinskyy, T. Roch, M. Truchlý, P. Švec, T. Huminiuc, T. Polcar, Structure, mechanical and tribological properties of mo-S-N solid lubricant coatings, Appl. Surf. Sci. 486 (2019) 1–14.
[32] J. Kalisz, K. Zak, S. Wojciechowski, M.K. Gupta, G.M. Krolczyk, Technological and tribological aspects of milling-burnishing process of complex surfaces, Tribol. Int. 155 (2021), 106770.
[33] W. Koszela, P. Pawlus, E. Rejwera, S. Ochwatb, Possibilities of oil pockets creation by the burnishing technique, Arch. Civ. Mech. Eng. 13 (2013) 465–471.
[34] N.S.M. El-Tayeb, K.O. Low, P.V. Brevern, On the surface and tribological characteristics of burnished cylindrical Al-6061, Tribol. Int. 42 (2009) 320–326.
[35] R. Khuengpukheiw, A. Wisitsoraat, C. Saikaew, Wear behaviors of HVOF-sprayed NiSiCrFeB, WC-Co/NiSiCrFeB and WC-Co coatings evaluated using a pin-on-disc tester with C45 steel pins, Wear 484-485 (2021), 203699.
[36] M. Olsson, S. Söderberg, S. Jacobson, S. Hogmark, Simulation of cutting tool wear by a modified pin-on-disc test, Int. J. Mach. Tools Manuf. 29 (1989) 377–390.
[37] E.S. Gadelmawla, M.M. Koura, T.M.A. Maksoud, I.M. Elewa, H.H. Soliman, Roughness parameters, J. Mater. Process. Technol. 123 (2002) 133–145.
[38] A. Dzierwa, A.P. Markopoulos, Influence of ball-burnishing process on surface topography parameters and tribological properties of hardened steel, Machine 7 (2019) 1–13.
[39] Begriffe Verschleiss, Systemanalyse von Verschleissvorgängen, Gliederung des, 1979.
[40] E. George, G.E. Kurien, U. Vishal, P.M. Anil, A study on the effect of oil pocket density on the effectiveness of boundary lubrication in the liner-ring interface, Procedia Eng. 64 (2013) 1062–1068.
[41] W. Koszela, A. Dzierwa, L. Galda, P. Pawlus, Experimental investigation of oil pockets effect on abrasive wear resistance, Tribol. Int. 46 (2012) 145–153.
[42] K. Oßwald, I. Lochmahr, Y. Bagci, P. Saile, Investigation into hand scraping: a microanalysis, J. Manuf. Mater. Process. 2 (2018) 76.
[43] C. Anderberg, F. Cabanettes, Z. Dimkovski, R. Ohlsson, B.-G. Rosén, Cylinder liners and consequences of improved honing, in: 12th Nordic Symposium on Tribology, 2006 (Degree Thesis).
[44] A. Kovalchenko, O. Ajayi, A. Erdemir, G. Fenske, I. Etsion, The effect of laser surface texturing on transitions in lubrication regimes during unidirectional sliding contact, Tribol. Int. 39 (2005) 219–225.
[45] X. Luo, J. Cao, G. Meng, Y. Chuan, Z. Yao, Hui xie: systematical investigation on the microstructures and tribological properties of fe-Al laser cladding coatings, Appl. Surf. Sci. 516 (2020), 146121.
[46] Y. Takashima, W. Natsu, Study on electrochemical machining of oil pocket on sliding surface with electrolyte suction tool, Procedia CIRP 42 (2016) 112–116.
[47] ISO 13565-2:1996 , Geometrical Product Specifications (GPS) — Surface Texture: Profile Method; Surfaces Having Stratified Functional Properties — Part 2: Height Characterization Using the Linear Material Ratio Curve.
[48] N. Allard, Consequences of Machining on Roughness and Functions of Cylinder liners surfaces, Högskolan i Halmstad/Sektionen för Ekonomi och Teknik, 2007. Dissertation.
[49] G. Mikoleizig, Surface roughness measurements of cylindrical gears and bevel gears on gear inspection machines, Gear Technol. (2015) 48–55.
[50] R.K. Whittaker, H.S. Hothi, A. Eskelinen, G.W. Blunn, J.A. Skinner, A.J. Hart, Variation in taper surface roughness for a single design effects the Wear rate in Total hip arthroplasty, J. Orthop. Res. 35 (2017) 1784–1792.
[51] ISO 25178-2:2012 , Geometrical Product Specifications (GPS) — Surface Texture: Areal — Part 2: Terms, Definitions and Surface Texture Parameters.
[52] Z. Dimkovski, Characterization of a Cylinder Liner Surface by Roughness Parameters Analysis Master's, Department of Mechanical Engineering Blekinge Institute of Technology, Karlskrona, Sweden, 2006 (Degree Thesis).
[53] D.J. Whitehouse, Handbook of Surface Metrology, CRC Press, United Kingdom, 2010.
[54] R. Horváth, Á. Drégelyi-Kiss, Gy. Mátyási, The examination of surface roughness parameters in the fine turning of hypereutectic aluminium alloys, UPB Sci. Bull. Ser. D: Mech. Eng. 77 (2015) 205–216.
[55] G.M. Krolczyk, J.B. Krolczyk, R.W. Maruda, S. Legutko, M. Tomaszewski, Metrological changes in surface morphology of high-strength steels in manufacturing processes, Measurement 88 (2016) 176–185.
[56] Zs. Kovács, Zs.J. Viharos, J. Kodácsy, The effects of machining strategies of magnetic assisted roller burnishing on the resulted surface structure, IOP Conf. Ser.: Mater. Sci. Eng. 448 (2018), 012002.
[57] F.J. Shiou, C.H. Cheng, Ultra-precision surface finish of NAK80 mould tool steel using sequential ball burnishing and ball polishing processes, J. Mater. Process. Technol. 201 (2008) 554–559.
[58] ISO 4288:1996 , Geometrical Product Specifications (GPS) — Surface Texture: Profile Method — Rules and Procedures for the Assessment of Surface Texture.
[59] Gy. Varga, J. Kundrák, Effects of technological parameters on surface characteristics in face milling, Solid State Phenom. 261 (2017) 285–292.